COLLAPSE ANALYSIS OF 4-STORY STEEL MOMENT-RESISTING FRAMES

Peng Pan[1], Makoto Ohsaki[2] and Jingyao Zhang[3]

[1] *Lecturer, Dept. of Civil Engineering, Tsinghua University, P. R. China*
[2] *Associate Professor, Dept. of Architecture and Architectural Engineering, Kyoto University, Japan*
[3] *Post-doctoral Research Fellow, Dept. of Architecture and Architectural Eng., Kyoto Univ., Japan*
E-mail: panpeng@mail.tsinghua.edu.cn, ohsaki@archi.kyoto-u.ac.jp, is.zhang@archi.kyoto-u.ac.jp

ABSTRACT :

A post-test analysis has been carried out for the shake-table test of a full-scale 4-story steel moment-resisting frame at E-Defense, Japan. The beams, columns and slabs are discretized to shell elements, and nonlinear time-history analysis is carried out by a commercial software package called ABAQUS. The numerical results are compared with the experimental results, and the effects of damping and stiffness on the responses are investigated.

KEYWORDS: Finite element analysis, Steel frame, Seismic response analysis, Collapse analysis

1. INTRODUCTION

Various numerical methods have been developed for time-history seismic response analysis of steel moment-resisting frames. It has been shown in many studies that elastoplastic behavior can be simulated accurately using two-dimensional frame model. However, it is important that the collapse behavior of steel frame should be simulated by fully taking into account the three-dimensional effects of input motions and response properties.

The purpose of this study is to investigate the accuracy of finite element elastoplastic dynamic analysis for predicting collapse behavior of a low-rise steel frame. Collapse analysis is carried out for the four-story frame model as the specimen of full-scale shake-table test (Suita *et al*., 2007) conducted in September 2007 at E-Defense shake-table facility, which is world's largest earthquake simulator. The test is one of the series of experimental studies on moment-resisting frames, innovative methods for new or existing buildings, protective systems, and nonstructural elements (Kasai *et al*., 2007).

In order to investigate the issues such as modeling techniques, estimation of damping and stiffness of nonstructural components, extensive computational studies are being conducted before and after the test by the members of the committee in charge of the test. Among several types of analysis described in Tada *et al*. (2007), the post-test analysis results by the finite element model using shell elements is reported in this study to investigate the effects of damping and stiffness on the collapse behavior.

2. FINITE ELEMENT MODEL

3D finite element analysis using a commercial code ABAQUS Ver. 6.5 (ABAQUS Inc., 2005) is carried out to simulate the shake-table test results of the four-story steel moment frame as shown in Figure 1. The details of the geometrical and mechanical properties of the frame is described in Suita *et al*. (2008). As shown in Figure 2, the beams, columns, and panel zones are modeled by the shell element S4R, which is a reduced-integration quadrilateral thick shell element considering shear deformation, and is applicable to large-strain deformation.

Fine mesh is used to model the portion that is prone to buckling and/or plastification (e.g.,

beam-to-column connections and column bases). Coarse mesh is adopted for remaining portions in order to reduce the computation time. Concrete slabs are also modeled by the S4R element, and are connected to beams through steel studs, where the composite action is modeled by a connector element CONN3D2, which is also used for the column bases.

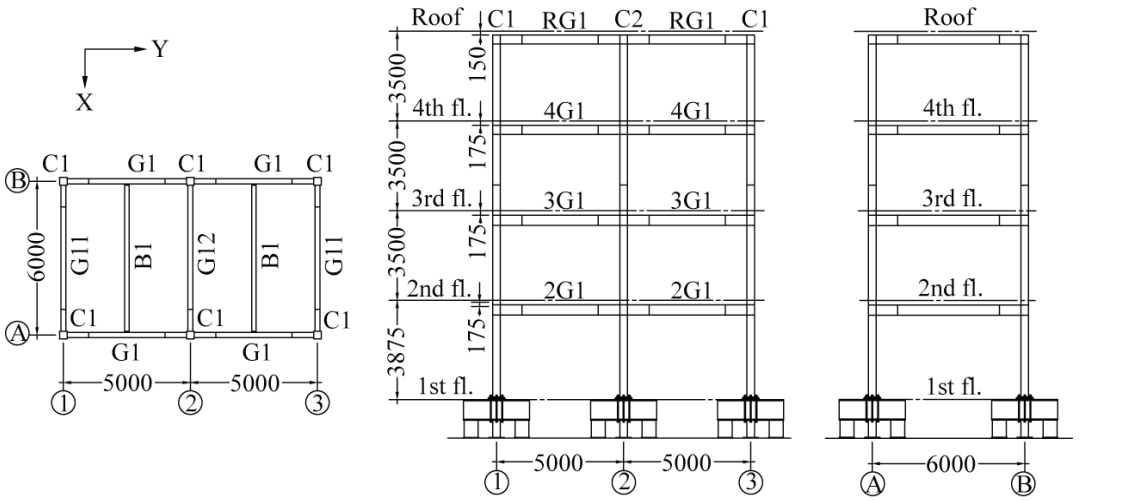

(a) Plan (1st Floor) (b) Y-Elevation (longitudinal) (c) X-Elevation (transverse)

Figure 1 Four-story steel moment frame.

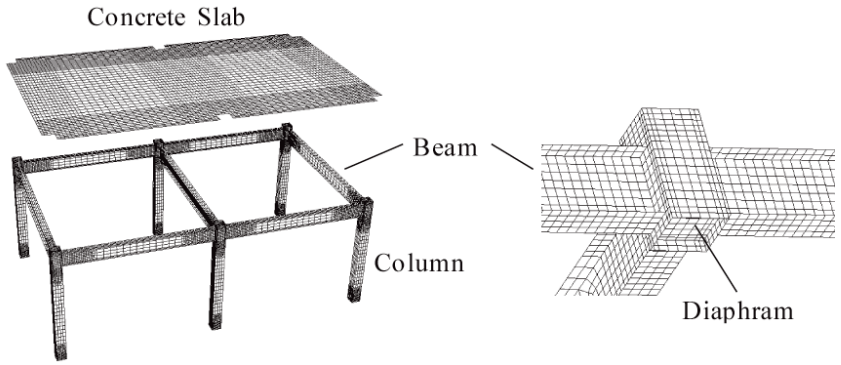

Figure 2 Finite element model by ABAQUS.

The hysteresis properties of the steel material is modeled by nonlinear kinematic/isotropic hardening obeying the J_2 associated flow theory with Ziegler's hardening rule. Young's modulus is 205.0 kN/mm^2, Poisson's ratio is 0.3, and mass density is 7800 kg/m^3. Figures 3 and 4 show the relation between stress and equivalent plastic strain of the materials of beams and columns, respectively, which have been obtained from the result of uniaxial coupon test (Suita *et al.*, 2008). The parameters for nonlinear hardening rule are automatically identified by assigning the stress-strain relation to the input file of ABAQUS.

The damage plasticity model is used for concrete material, where Young's modulus is 20.11 kN/mm^2 and Poisson's ratio is 0.2. The yield stress is –18.0 N/mm^2 for compression and 2.3 N/mm^2 for tension. Note that very small damage parameters are given to improve convergence property of the analysis process. Therefore, the stress-strain retation of concrete is almost bilinear with different yield stresses in compression and tension. The relation between the rotation and the moment of the spring at the column base has a bilinear elastic-plastic constitutive law, where the initial stiffness is 4.891×10^4 kNm, the yield moment is 604.2 kNm, and the hardening coefficient is 1/100.

The numbers of elements and nodes are 75,082 and 79,684, respectively, and the total number of variables, which is the sum of the number of degrees of freedom of nodal displacements and Lagrange multipliers for constrained DOFs by the connector elements, is 456,750. A direct sparse solver is adopted for solving linear equations. Computation is carried out on a personal workstation with AMD Opteron 2.6 GHz (2 CPUs) with 2GB memory.

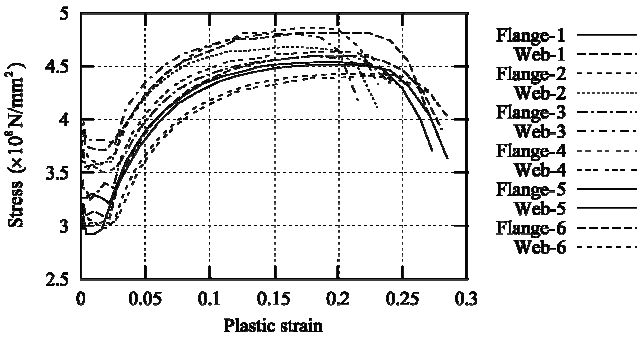

Figure 3 Material property of beam.

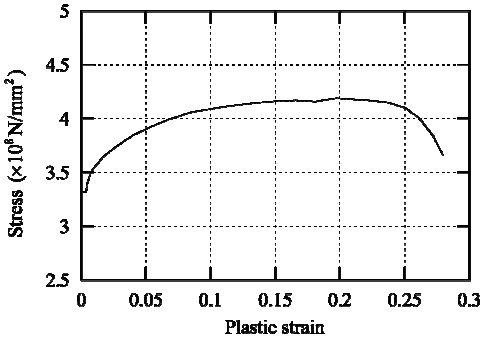

Figure 4 Material property of column.

3. TIME-HISTORY ANALYSIS.

To avoid the unrealistic local stress concentration, the story mass is distributed to the nodes of the slab; i.e., the mass density of the slab is computed from the assigned story mass divided by the volume of the slab. The computed mass densities (kg/m^3) are 5041.30, 5138.48, 5272.11 and 7312.93, respectively, for 2nd, 3rd, 4th floors and the roof. Static analysis is carried out before time-history analysis to apply the gravity load to the frame.

The periods (sec.) of the four lowest modes are 1.050, 0.999, 0.705 and 0.328. The first three modes correspond to X-directional, Y-directional, and torsional lowest modes, respectively, and the fourth mode is the second lowest in X-direction. Rayleigh damping is adopted, where the damping ratios are 0.02 for the first and fourth modes. The input accerelations are the 1995 Hyogoken-Nanbu Earthquake Takatori wave that are scaled to various levels. However, the actual acceleration records in three directions measured on the shake-table during the series of tests are used as the input acceleration. Newmark-β method (β =1/4) is used for the time integration scheme. The maximum time step size is 0.02 sec., which is reduced automatically when extensive plastification and/or instability occurrs.

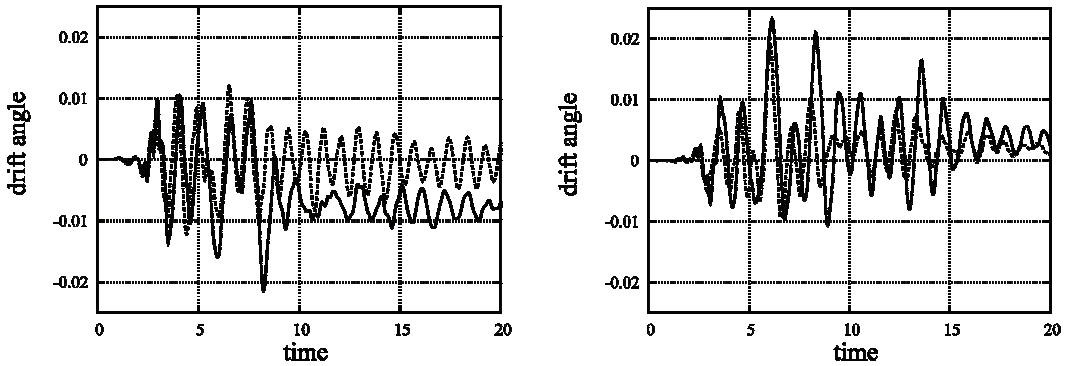

(a) X-direction (b) Y-direction

Figure 5 Time history of drift angles of the 1st story for 60%-Takatori; h = 0.02, K = 1.0.

We computed the responses of the structure with various levels of damping ratio h and stiffness parameter K, where h = 0.02 for 1st and 4th modes and K = 1.0 represent the original model. Time

histories of the 1st-story drift angles in X- and Y-directions for h = 0.02 and K = 1.0 are plotted in solid lines in Figure 5, where the target motion is the Takatori wave scaled by 0.6, which is designated as the incipient-collapse level motion. The dotted lines are the measured responses by experiment, which show that the numerical results significantly overestimate the experimental results. This is supposed to be mainly caused by underestimation of damping and stiffness due to the nonstructural components. The relations between drift angle and shear force in X- and Y- directions of the 1st story are ploted in Figure 6. The ratios of the computed values to experimental results of maximum absolute values of story drift angles and story shears of 1st story are listed in Table 1. As is seen in the row of h = 0.02 and K = 1.0, the story shear is slightly (4%) underestimated in X-direction and significantly (27%) underestimated in Y-direction. Note that the spring in the column-base remaines in elastic range for this analysis.The CPU time for static and dynamic analysis is 43.3 hrs.

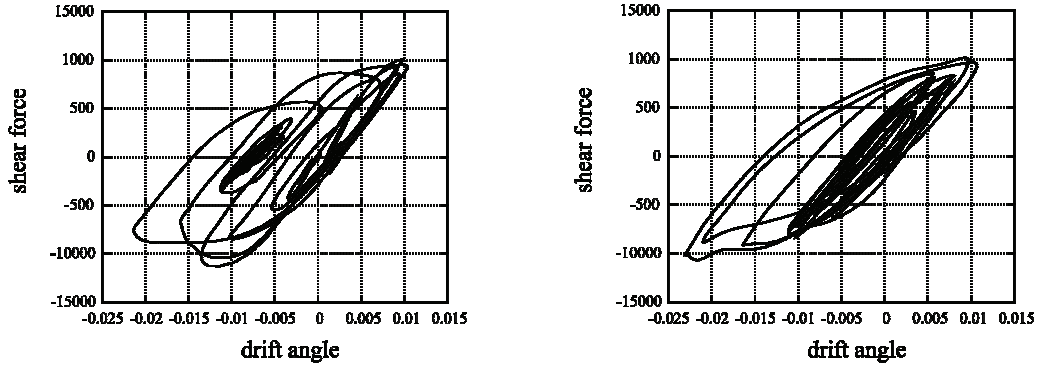

(a) X-direction (b) Y-direction

Figure 6 Shear forces and drift angles of the 1st story for 60%-Takatori; h = 0.02, K = 1.0.

Table 1 Ratios of computed values to experimental results of maximum absolute values of story drift angles and story shears of 1st story.

		Drift angle		Story shear	
		X-dir.	Y-dir.	X-dir.	Y-dir.
40%-Takatori	h = 0.02, K = 1.0	1.04	0.79	0.98	0.71
60%-Takatori	h = 0.02, K = 1.0	1.73	1.20	0.96	0.73
	h = 0.05, K = 1.0	1.18	0.85	0.92	0.71
	h = 0.02, K = 1.1	1.17	0.81	0.91	0.73

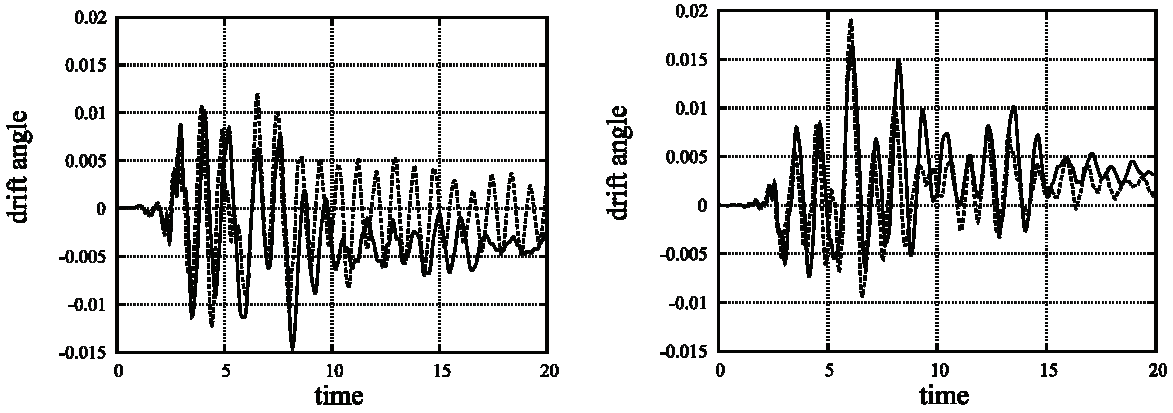

(a) X-direction (b) Y-direction

Figure 7 Time history of drift angles of the 1st story for 60%-Takatori; h = 0.05, K = 1.0.

To incorporate the damping effect of the nonstructural components, time histories of the 1st story drift angles in X- and Y-directions for the increased Rayleigh damping with 0.05 for 1st and 4th modes (h =

0.05 and K = 1.0) are plotted in Figure 7 for the same incipient-collapse level motion. The dotted lines are the measured responses by experiment. As is seen from Figure 7 and Table 1, the predicted maximum absolute values of drift angles have better agreement to the experimental results than the case of smaller damping in Figure 5. Therefore, the response to the seismic motion of incipient-collapse level is very sensitive to the damping ratio, and accurate estimate of damping, mainly due to nonstructural components, is critical for good estimate of elastoplastic responses. The relations between drift angle and shear force in X- and Y- directions of the 1st story are ploted in Figure 8. The maximum shear force is also underestimated, mainly in Y-direction, also for this case as shown in Table 1.

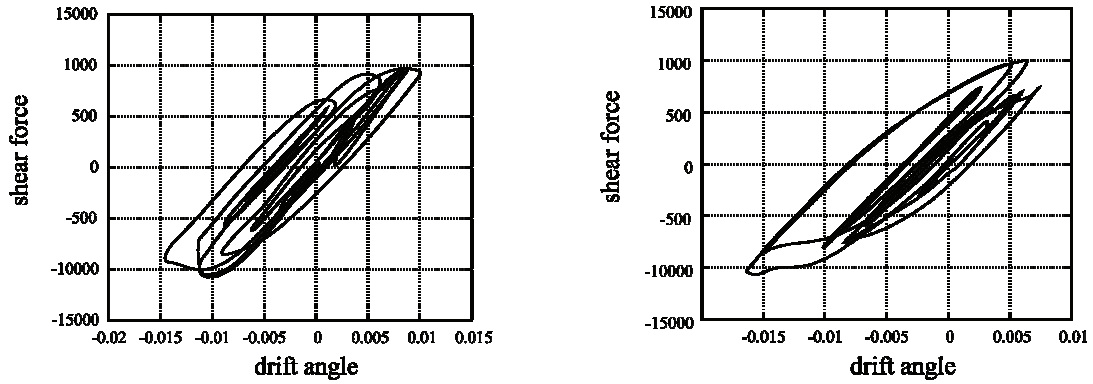

(a) X-direction (b) Y-direction

Figure 8 Shear forces and drift angles of the 1st story for 60%-Takatori; h = 0.05, K = 1.0.

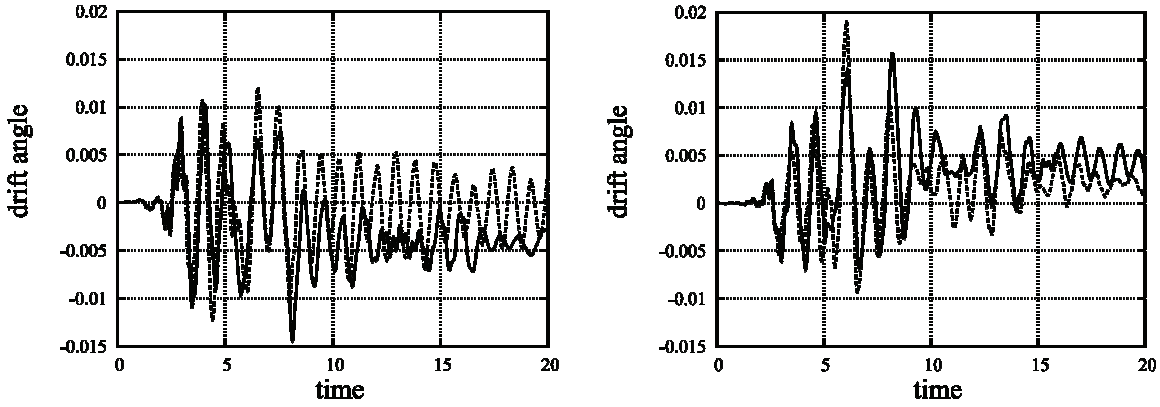

(a) X-direction (b) Y-direction

Figure 9 Time history of drift angles of the 1st story for 60%-Takatori; h = 0.02, K = 1.1.

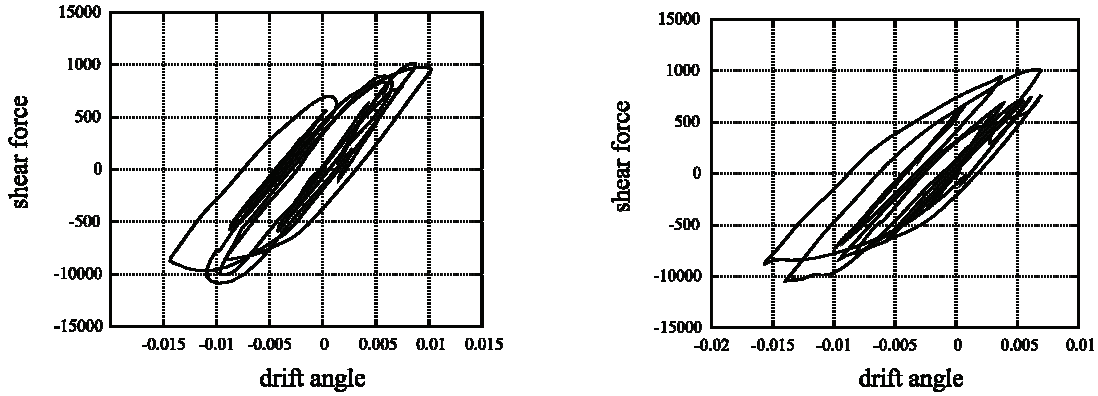

(a) X-direction (b) Y-direction

Figure 10 Shear forces and drift angles of the 1st story for 60%-Takatori; h = 0.02, K = 1.1.

Next, in order to incorporate the stiffness of the nonstructural components, Young's modulus of steel is increased by the factor 1.1 without changing the damping ratio; i.e., h = 0.02 and K = 1.1. The time histories of the 1st-story drift angles in X- and Y-directions are plotted in Figure 9 for the incipient-collapse level motion. As is seen from Figure 9 and Table 1, the predicted maximum absolute values of drift angles have better agreement to the experimental results than the original model. Therefore, the response to the seismic motion of incipient-collapse level is very sensitive also to the stiffness of the frame, and accurate estimate of the stiffness of nonstructural components is critical for good estimate of elastoplastic responses. The relations between drift angle and shear force in X- and Y-direction of the 1st story are ploted in Figure 10. The maximum shear force is also underestimated, mainly in Y-direction, also for this case as shown in Table 1.

Figure 11 shows the time histories of the 1st-story drift angles in X- and Y-directions for the target Takatori wave scaled by 0.4 for the original model (h = 0.02 and K = 1.0). The relations between drift angle and shear force in X- and Y- directions of the 1st story are ploted in Figure 12. As is seen from these results and Table 1, the responses are more accurately estimated, mainly in X-direction, than those of the target Takatori wave scaled by 0.6. Therefore, the effect of nonstructural components is not very significant in this case .

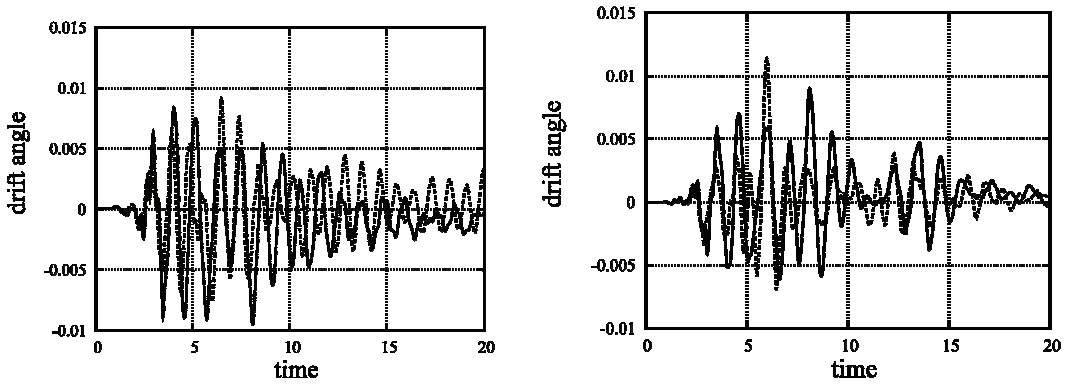

(a) X-direction (b) Y-direction

Figure 11 Time history of drift angles of the 1st story; input level: 0.4. damping: 0.02.

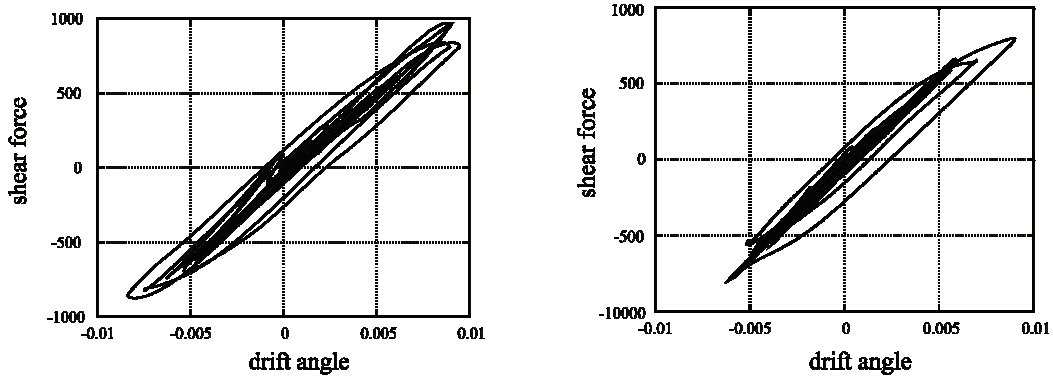

(a) X-direction (b) Y-direction

Figure 12 Shear forces and drift angles of the 1st story for 40%-Takatori; h = 0.02, K = 1.0.

Figure 13 shows the time histories of the 1st-story drift angles in X- and Y-directions for the collapse-level target Takatori wave without scaling for the original model (h = 0.02 and K = 1.0). The relations between drift angle and shear force in X- and Y- direction of the 1st story are ploted in Figure 14. As is seen from these results, good agreement is observed in the collapse times of the computational and experimental results, when the maximum drift angle in Y-direction reached 0.13 rad. Therefore, the

effect of nonstructural components is not very significant also in this case .

The deformation in real scale of the whole frame, 2nd floor level around the internal column, and the base of the internal column at the collapse state are shown in Figure 15, where the contour lines represent the von Mises stress. As is seen, the local failure and the global collapse behavior are simultaneously simulated by the finite element analysis using shell elements. The collapse behavior due to the mechanism in the 1st story and the direction of collapse are very similar to those in the experiment.

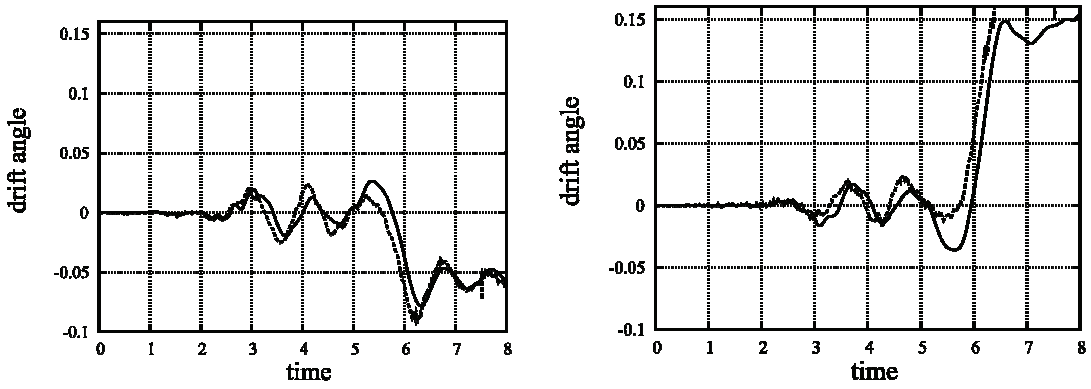

(a) X-direction (b) Y-direction

Figure 13 Time history of drift angles of the 1st story for 100%-Takatori; $h = 0.02$, $K = 1.0$.

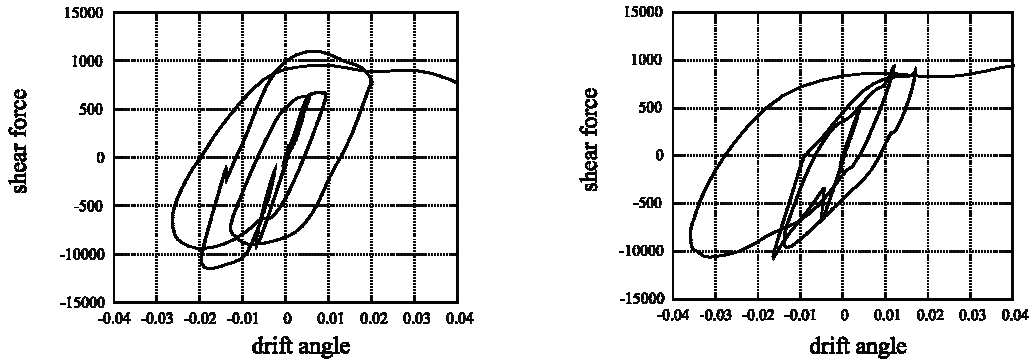

(a) X-direction (b) Y-direction

Figure 14 Shear force and drift angles of the 1st story for 100%-Takatori; $h = 0.02$, $K = 1.0$.

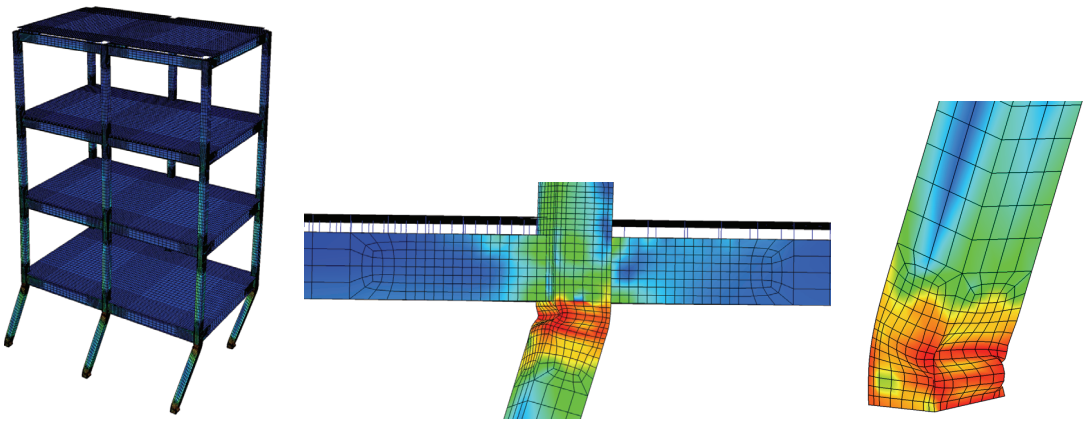

Figure 15 Deformation in real scale of the whole frame, 2nd floor level around the internal column, and the base of the internal column at the collapse state.

4. CONCLUSIONS

Elastoplastic dynamic analysis has been carried out for the four-story steel moment-resisting frame that is the specimen of the shake-table test at E-Defense, Japan. The measured acceleration on the shake-table is used as the input acceleration. The beams and columns are discretized to shell elements to simulate the local buckling and plastification. It has been shown that the local failure and the global collapse behavior are simultaneously simulated by the finite element analysis using shell elements.

Although good agreement has been observed in the responses against the collapse-level seismic motion, the responses against the incipient-collapse level strongly depend on the damping ratio and the stiffness of the structure due to the existence of nonstructural components. More accurate constitutive relation should also be used for the reinforced concrete for the slabs and the column bases.

ACKNOWLEDGEMENTS

This study is a part of "NEES/E-Defense collaborative research program on steel structures," and was pursued by the Analysis Method and Verification WG. The Japan team leader for the overall program is Kazuhiko Kasai, Tokyo Institute of Technology, and the WG leader is Motohide Tada, Osaka University. The authors acknowledge the support by the members of Building Collapse Simulation WG (leader: Keiichiro Suita, Kyoto University), and the financial support provided by the National Research Institute for Earth Science and Disaster Prevention.

REFERENCES

ABAQUS Ver. 6.5 Documentation, ABAQUS Inc., 2005.

Kasai, K., Ooki, Y., Motoyui, S., Takeuchi, T. and Sato, E. (2007). E-Defense tests on full-scale steel buildings: Part 1 – Experiments using dampers and isolators, Proc. Structural Congress 2007, ASCE, Long Beach, 247-17.

Suita, K., Yamada, S., Tada, M., Kasai, K., Matsuoka, Y. and Sato, E. (2007) E-Defense tests on full-scale steel buildings: Part 2 – Collapse experiments on moment frames, Proc. Structural Congress 2007, ASCE, Long Beach, 247-18.

Suita, K., Yamada, S., Tada, M., Kasai, K., Matsuoka Y. and Sato, E. (2008). E-Defense tests on full-scale steel buildings: Part 1 – Analytical simulation of collapse, Proc. Structures Congress 2008, ASCE, Vancouver.

Tada, M., Ohsaki, M., Yamada, S., Motoyui, S. and Kasai, K. (2007). E-Defense tests on full-scale steel buildings: Part 3 – Analytical simulation of collapse, Proc. Structures Congress 2007, ASCE, Long Beach, 247-19.